PHYSICAL REVIEW E **83**, 065302(R) (2011)

# Flow coupling during three-phase gravity drainage

H. Dehghanpour, B. Aminzadeh, M. Mirzaei, and D. A. DiCarlo*

*Department of Petroleum and Geosystems Engineering, The University of Texas at Austin, Austin, Texas 78712, USA*

(Received 15 June 2010; revised manuscript received 16 November 2010; published 20 June 2011)

We measure the three-phase oil relative permeability $k_{ro}$ by conducting unsteady-state drainage experiments in a 0.8 $m$ water-wet sand pack. We find that when starting from capillary-trapped oil, $k_{ro}$ shows a strong dependence on both the flow of water and the water saturation and a weak dependence on oil saturation, contrary to most models. The observed flow coupling between water and oil is stronger in three-phase flow than two-phase flow, and cannot be observed in steady-state measurements. The results suggest that the oil is transported through moving gas-oil-water interfaces (form drag) or momentum transport across stationary interfaces (friction drag). We present a simple model of friction drag which compares favorably to the experimental data.

DOI: 10.1103/PhysRevE.83.065302 PACS number(s): 47.56.+r, 47.55.Ca, 47.55.nd, 89.30.aj

When the single-phase Darcy equation is generalized to multiphase flow in porous media, it is assumed that each phase flows due to the pressure gradient within that phase, albeit with a reduced permeability [1,2]. Conceptually, each phase flows in a capillary-stable reduced network compared to single phase flow. The change in permeability is parameterized by the relative permeability $k_{ri}$ that is assumed to be a function of the phase saturation $S_i$ [the local volume fraction of the pore space filled by the phase $i$, where $i = o$ (oil), $w$ (water), $g$ (gas)]. Mathematically this is expressed through the Darcy-Buckingham equation [1]

$$q_i = -k\frac{k_{ri}(S_i)}{\mu_i}\left(\frac{dP_i}{dz} + \rho_i g\right). \tag{1}$$

Here, $q_i$, $\mu_i$, $\rho_i$, and $P_i$ are the flux, viscosity, density, and pressure of phase $i$ flowing through porous media of permeability $k$. While this multiphase flow equation is widely used due to its simplicity, it is known to break down at high capillary numbers (the network is fluid) [3], unstable flow [4], high viscosity ratio (due to viscous coupling between the mobile phases) [5], and three-phase flow (the network for the intermediate phase depends on the other two phases) [6].

Here we concentrate on the combined effects of three-phase flow and viscous coupling. Three-phase flow occurs when three mobile fluid phases coexist in a porous media; typically water is the most wetting phase and oil the intermediate wetting phase. Three-phase relative permeability has been measured using steady-state experiments [6], and many empirical models of the oil relative permeability $k_{ro}$ have been introduced [7]. These models have a dependence on both saturations $k_{ro}(S_o, S_w)$, based on the idea that the connected oil network depends on the amount of water. From observations in micromodels [8,9] and capillary stability arguments based on geometry [10] and thermodynamics [11] various three-phase pore level fluid configurations and flow mechanisms have been recognized. These mechanisms have been incorporated into network models to predict three-phase relative permeability and saturations path [12–14], under the ansatz of each phase flowing independently in its own network.

Viscous coupling, where the pressure gradient of a particular phase affects the flow of the other phase, has been investigated for two-phase flow through experiments [15–17], analytical calculations [18,19], and simulations at the pore scale [20].

In this Rapid Communication we conduct three-phase gravity drainage experiments with different initial conditions and measure the *in situ* saturations versus space and time (see schematic in Fig. 1) from which we obtain $k_{ro}$ and $k_{rw}$. The observed dependencies of the relative permeabilites suggest that flow coupling dominates $k_{ro}$ for a significant portion of three-phase flow. We propose a simple physical model from which the flow coupling can be solved for exactly, and find that the dependencies of this solution qualitatively matches the experiments.

The porous medium consisted of an 80-cm column of sand pack (dry continuous pack) inside a rubber sleeve with an inner diameter of 7.5 cm. The confining pressure of 50 psi was provided by water to prevent flow near the edge. The mean particle size, average porosity, and permeability of the water wet sand pack were 0.25 mm, 0.3, and $6 \times 10^{-12}$ m$^2$, respectively. A 10 wt% aqueous solution of NaBr, $n$-octane, and air were used as water, oil, and gas, respectively. The density and viscosity of the oil phase is 703 kg/m$^3$ and 0.51 cP and that of the aqueous phase is 1069 kg/m$^3$ and 1.23 cP. The interfacial tensions (mN/m) between fluid pairs are $\sigma_{go} = 21.4$, $\sigma_{gw} = 72$, and $\sigma_{ow} = 51.5$ yielding an initial spreading coefficient of the oil on water of $S = -0.8$ and a final spreading coefficient (after the three phases equilibrate) of $S = -1.9$ [21]. Theoretical arguments backed with micromodel observations show that nearly spreading oils like $n$-octane form intermediate layers in the crevices of the pore space [22].

The initial condition of tests 1 and 2 were oil filled with residual water saturation. These were produced by injecting one pore volume of oil from the top of the column fully saturated with water (test 1) and saturated with water and trapped gas (test 2). The initial condition of tests 3 and 4 were water filled with residual oil saturation. These were produced by injecting one pore volume of water from the bottom of the column saturated with oil, trapped gas, and residual water. The initial condition of test 5 was produced by co-injection of oil (5 mL/min) and water (8 mL/min) from the

*dicarlo@mail.utexas.edu

 

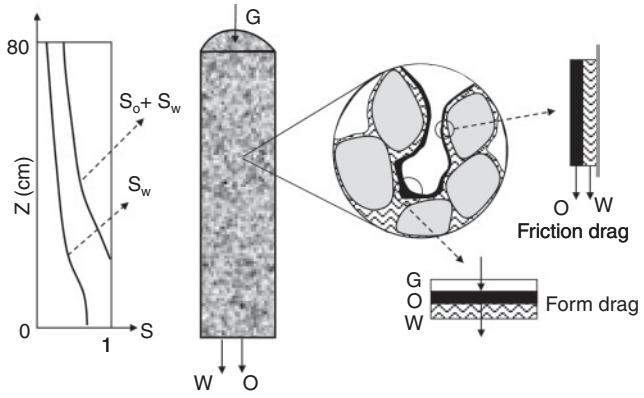


FIG. 1. Schematic illustration of the experimental setup and pore level displacement mechanisms. Center: Gas invades the column, initially saturated with oil and water, from the top, and oil and water are produced from the bottom. Left: The two curves indicate the macroscopic saturation of oil and water in space at a particular time. Right: Microscopically, oil layers are sandwiched between water and gas, and the layers are stabilized by capillary forces. Momentum is transferred to oil through friction and form drag.

top of the column. The drainages began by opening the bottom valve and the system drained naturally under the gravity. For tests 1 through 3 the drainages began 24 hours after the last flood, and for tests 4 and 5 the drainages began immediately after setting the initial condition.

A modified medical CT scanner was used to obtain fluid saturations versus time and space during the drainage. The length of the column was scanned at two different tube energy levels (130 and 80 kV). Each image was integrated to get an average CT attenuation number at each height. For each image, the high and low energy CT values are converted into saturations for water, oil, and gas ($S_w$, $S_o$, and $S_g$, respectively) using the two independent linear attenuation equations [23]. The Br ions in the water phase preferentially attenuate the low energy x rays, allowing a discrimination between the water and oil phases. Figure 2 shows the saturation data in time and space measured during test 4. The inset in Fig. 2(a) shows a blow up of the oil data, and from the repeatability we estimate we can resolve changes in $S_o$ and $S_w$ down to 0.003.

From the *in situ* saturations versus time and space, we use the method first suggested by Watson [24] to calculate the relative permeability of the water and oil. Equation (1) can be

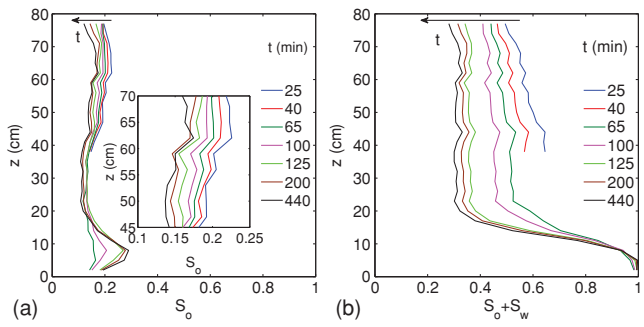


FIG. 2. (Color online) (a) Measured oil saturation in time and space for test 4. (b) Measured liquid saturation $S_o + S_w$ for the same test.

rearranged to obtain the three-phase relative permeability of oil $k_{ro}$ as a function of the flux and corresponding driving force $\rho_o g + dP_o/dz$. We use the observation that behind the main drainage front [$40 < z < 70$, see Fig. 2(b)] the gas saturation gradient is very low, $dS_g/dz \leqslant 0.002\ \mathrm{cm}^{-1}$, which, when using the static capillary pressure curve, corresponds to $d(P_g - P_o)/dz \leqslant 0.03\rho g$. Making the typical assumption that the gas pressure gradient is negligible, in this region $dP_o/dz \ll \rho g$ and can be ignored. Thus the relative permeability of oil is simply given by $k_{ro}(z,t) = (\mu_o/k\rho_o g)q_o(z,t)$. The flux of oil at a particular time and location $q_o(z,t)$ is obtained by integrating between two consecutive saturation profiles from the top of the column.

Unlike the steady-state method which proscribes certain flow ratios, the unsteady-state method for measuring $k_{ro}$ and $k_{rw}$ allows the flow to develop organically. The saturation path, the fluxes, and the rates of saturation change are all allowed to affect $k_{ro}$ and $k_{rw}$. Figure 3 shows the local $k_{ro}$ plotted versus the local $S_o$ at each time and position for all five drainages along with the curve obtained from two-phase gas-oil drainages $k_{ro}^{2ph}$. Each drainage produces roughly 100 data points. Comparing the three-phase results to the two-phase results, we observe that when draining from residual water (tests 1 and 2) $k_{ro} \approx k_{ro}^{2ph}$ for $S_o > 0.18$. For $S_o < 0.18$, $k_{ro} > k_{ro}^{2ph}$ due to the formation of oil layers on top of the residual water, and has been observed previously [6].

More interesting are the measured $k_{ro}$ data starting from two-phase oil-water residual oil $S_o \approx 0.18$ (tests 3 and 4). Before the gas is allowed to invade, the oil is immobile and necessarily $k_{ro} = 0$. But when gas enters the column, $k_{ro}$ jumps to $k_{ro} > 3 \times 10^{-2}$. At $S_o \approx 0.18$, $k_{ro}$ is two orders of magnitude greater than the measured $k_{ro}^{2ph}$ and $k_{ro}$ from

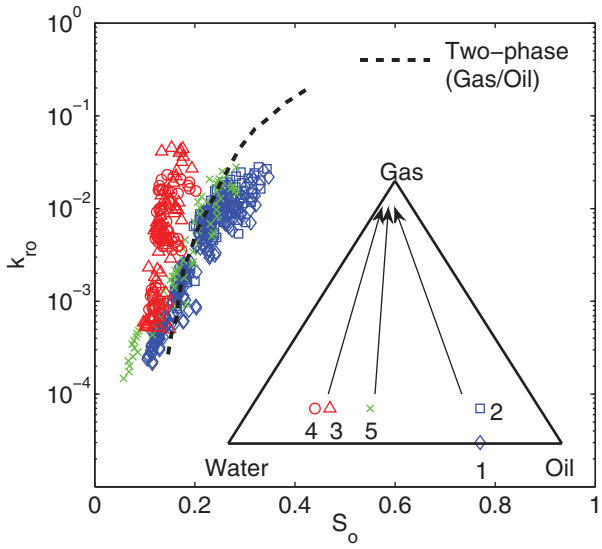


FIG. 3. (Color online) Three-phase oil relative permeability measured during gravity drainage. Each symbol depicts a different drainage, the total number of symbols are for all of the positions and times measured. The dashed line depicts the oil relative permeability obtained from a two-phase gas-oil drainage. Inset: The initial condition and saturation path related to each test is schematically shown in the ternary plot.

tests 1 and 2 starting at residual water saturation. As the drainage proceeds, $k_{ro}$ decreases rapidly, but with very small changes in corresponding $S_o$. This is counter to most models of relative permeability, which have the relative permeability depending strongly on the saturation of the particular phase. Finally, drainages that start from an intermediate oil and water saturations (x's), show $k_{ro}$ between the two endpoint cases.

Figure 4(a) shows the measured $k_{ro}$ of tests 3 and 4 as a function of $S_o$ and $S_w$. The open symbols are the same data presented in Fig. 3, namely $k_{ro}$ as a function of $S_o$, and there is only a weak correlation of $k_{ro}$ on $S_o$. When the same data are plotted as a function of $S_w$, we observe a strong correlation between $k_{ro}$ and $S_w$. This suggests that on the remobilization of oil, the key saturation variable is $S_w$ and not $S_o$.

We examine this effect further in the inset of Fig. 4(a), where we plot the same $k_{ro}$ but as a function of $k_{rw}$, where $k_{rw}$ is basically the measured flux of water $q_w$ multiplied by $\mu_w/(k\,\rho_w\,g)$. Here we observe a strong correlation between $k_{ro}$ and $k_{rw}$ over three orders of magnitude. These data lend themselves to the conclusion that the relative oil flow (through $k_{ro}$) is influenced much more by the water flux (or, equivalently, the water saturation as at high water saturation $k_{rw}$ is a function of $S_w$) than by the local saturation of oil. Simply, the oil flow is coupled to the water flow. Heuristically, this coupling can be through two different physical mechanisms depicted in Fig. 1: (a) a double drainage mechanism where the oil is transported in moving gas-oil-water interfaces, (b) the direct transfer of momentum from the moving water phase to the oil phase through stationary water-oil interfaces. We will explore these in turn.

Upon gas invasion, the invading gas reconnects the trapped oil, which spreads between the gas and water. On drainage, first the oil displaces the water followed by the gas displacing the oil. This double drainage mechanism has been observed in two-dimensional micromodels [8] and simulated at the pore scale [12,13], but has not been quantified in real porous media. One can think of this type of flow coupling mechanism as a type of form drag as the oil is dragged with the moving gas-oil and oil-water interfaces on drainage, and requires a change in local saturation with time $dS_w/dt$.

For the direct momentum transfer mechanism, consider water stabilized by capillary forces in the corners of the pore space, and oil in the form of layers between the gas and the water (see Fig. 1). In the geometrically complex pore space, these oil layers will be stabilized by capillary forces [12] and the water and oil will flow through these continuous layers by gravity. In this configuration, the oil will be dragged by the flowing water due to momentum transfer at the quasistationary oil-water interface as a type of friction drag. This is the model for traditional viscous coupling studied in two-phase systems, as the local saturation changes slowly with time [15]. This friction type of coupling should be greater in three-phase than two-phase systems as the oil in layers has a larger surface area to volume than the oil in bulk.

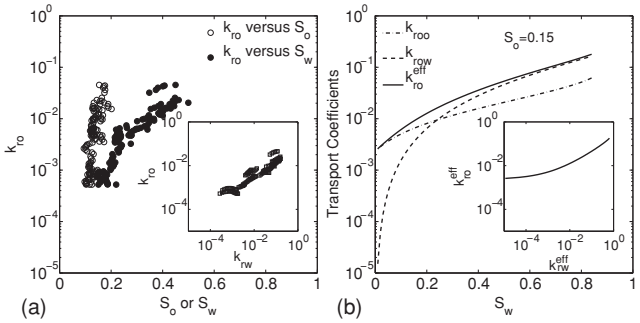


FIG. 4. (a) $k_{ro}$ measured during tests 3 and 4, versus $S_o$ and $S_w$. Inset: The same $k_{ro}$ data versus corresponding $k_{rw}$. (b) Calculated transport coefficients of the oil phase from the proposed model when $S_o = 0.15$ versus $S_w$. Inset: $k_{ro}^{\text{eff}}$ versus $k_{rw}^{\text{eff}}$ from the same model when $S_o = 0.15$

To model this phenomenon one needs to solve the three-phase creeping flow in capillary stable flow configurations such as the corners of a triangle. The conductance of the oil layers in corners has been studied experimentally and numerically [25–27], although these numeric models explicitly do not conserve momentum across the water-oil interface. Instead, for simplicity, we propose an idealized capillary tube model where the momentum can be analytically calculated. This model consists of a single circular capillary tube with water wetting the inner surface of the capillary, gas in the center, and an oil layer between water and gas. This is similar to the model of Rose [28] and Bacri [29] who derived the generalized relative permeability coefficients for two-phase (oil-water) flow in a circular capillary tube. Although not necessarily capillary stable, this is the simplest calculation of viscous coupling in three-phase flow.

We solve the above boundary value problem for water and oil domain by neglecting the nanoscale slip effect [30] and assuming continuity of velocity and shear stress at the water-solid and oil-water interfaces. The shear stress at the oil-gas interface is assumed to be zero. We consider the solution of this problem in the following form:

$$\begin{bmatrix} q_w \\ q_o \end{bmatrix} = k \begin{bmatrix} k_{rww} & k_{rwo} \\ k_{row} & k_{roo} \end{bmatrix} \begin{bmatrix} (d\phi_w/dz)/\mu_w \\ (d\phi_o/dz)/\mu_o \end{bmatrix}. \tag{2}$$

Here the flux of each phase is related to the gradient of the potential $\phi$ of both liquid phases by the transport coefficients ($k_{rij}$). By comparison between the solution of Stokes equation and suggested coupled Darcy Eq. (2), the four transport coefficients are given by

$$k_{roo} = S_o^2 \left[1 - 2\frac{\mu_o}{\mu_w}\ln(1-S_w)\right] - 2S_oS_g - 2S_g^2 \ln\left(\frac{S_g}{1-S_w}\right) \tag{3}$$

$$k_{rww} = S_w^2 - 2S_w(1-S_w) - 2(1-S_w)^2\ln(1-S_w), \tag{4}$$

$$k_{row} = k_{rwo}\left(\frac{\mu_w}{\mu_o}\right) = 2[S_o(1-S_w)\ln(1-S_w) + S_oS_w]. \tag{5}$$

Experimentally, the $q_o$ (and thus $k_{ro}$) that is measured will be a result of contributions from both $k_{roo}$ and $k_{row}$. We sum the following two to get the effective relative permeability of oil in a three-phase falling film problem $k_{ro}^{\text{eff}} = k_{roo} + (\rho_w\mu_o/\rho_o\mu_w)k_{row}$. Figure 4(b) shows the calculated transport coefficients for constant oil saturation of 0.15 as a function of water saturation. The standard description of three-phase flow states that $k_{ro}$ will increase with increasing $S_w$ as the oil will move to the center of the pore space reducing the friction.

This is observed in this simple model as $k_{roo}$ increases with increasing $S_w$. But above $S_w < 0.25$, the primary contribution to the oil flow $k_{ro}^{\text{eff}}$ is through the pressure gradient in the water ($k_{ow}$). Simply with increasing $S_w$, the water layer is thicker and oil flows on a faster moving boundary; this causes $k_{ro}^{\text{eff}}$ to increase by two orders of magnitude at constant $S_o$.

This simple model of $k_{ro}^{\text{eff}}$ can be compared to the data presented in Fig. 4(a). They show a similar order of magnitude and dependence on $S_w$. The inset of Fig. 4(b) presents the dependence of $k_{ro}$ on $k_{rw}$ in the same matter as the inset of Fig. 4(a). In a real porous media, there will be issues of pore-size distribution, connectivity, and capillary stable fluid arrangements that are much more complicated than this simple model, although the comparisons between the simple model and the results are suggestive.

As noted earlier, traditional three-phase models have $k_{ro}(S_o, S_w)$, and these results can be shoehorned into this framework, but only if hysteresis is added to $k_{ro}$.

In summary, both dynamic experiments and simple physical arguments show that for three-phase flow, the flow of the intermediate wetting phase is strongly coupled to the flow of the most wetting phase. Several physical mechanisms for the flow coupling are proposed, and experiments and modeling are continuing to delineate the exact nature of this coupling. These results suggest that predictions of three-phase flow at low oil saturations must take into account the flow of the other phases.

We thank N. Hajari, R. Johns, and L. Lake for discussions. H.D. and M.M. acknowledge support from the Industrial Associates Gas Flooding Program at The University of Texas at Austin. B.A. and D.D. acknowledge support from the Center for Frontiers of Subsurface Energy Security, an Energy Frontier Research Center funded by the US Department of Energy, Office of Basic Energy Sciences under Award No. DE-SC0001114.

[1] J. Bear, *Dynamics of Fluids in Porous Media* (American Elsevier, New York, 1972).
[2] F. A. L. Dullien, *Porous Media Fluid Transport and Pore Structure*, 2nd ed. (Academic Press, San Diego, CA, 1992).
[3] K. T. Tallakstad, H. A. Knudsen, T. Ramstad, G. Lovoll, K. J. Maloy, R. Toussaint, and E. G. Flekkoy, Phys. Rev. Lett. **102**, 074502 (2009).
[4] L. Cueto-Felgueroso and R. Juanes, Phys. Rev. Lett. **101**, 244504 (2008).
[5] A. S. Odeh, J. Pet. Technol. **11**, 346 (1959).
[6] M. J. Oak, L. E. Baker, and D. C. Thomas, J. Pet. Technol. **42**, 1054 (1990).
[7] L. Oliveira and A. H. Demond, J. Contam. Hydrol. **66**, 261 (2003).
[8] P. E. Oren and W. V. Pinczewski, Transp. Porous Media **20**, 105 (1995).
[9] P. E. Oren, J. Billiotte, and W. V. Pinczewski, SPE Form. Eval. **7**, 70 (1992).
[10] M. H. Hui and M. J. Blunt, J. Phys. Chem. B **104**, 3833 (2000).
[11] M. I. J. van Dijke and K. S. Sorbie, J. Colloid Interface Sci. **293**, 455 (2006).
[12] D. H. Fenwick and M. J. Blunt, Adv. Water Resour. **21**, 121 (1998).
[13] M. Piri and M. J. Blunt, Phys. Rev. E **71**, 026302 (2005).
[14] M. I. J. van Dijke and K. S. Sorbie, Phys. Rev. E **66**, 046302 (2002).
[15] F. A. L. Dullien and M. Dong, Transp. Porous Media **25**, 97 (1996).
[16] R. G. Bentsen and A. A. Manai, Transp. Porous Media **11**, 243 (1993).
[17] D. G. Avraam and A. C. Payatakes, Transp. Porous Media **20**, 135 (1995).
[18] S. Whitaker, Transp. Porous Media **1**, 105 (1986).
[19] F. Kalaydjian, Transp. Porous Media **2**, 537 (1987).
[20] H. Li, C. Pan, and C. T. Miller, Phys. Rev. E **72**, 026705 (2005).
[21] D. Zhou and M. J. Blunt, J. Contam. Hydrol. **25**, 1 (1997).
[22] M. Dong, F. A. Dullien, and I. Chatzis, J. Colloid Interface Sci. **172**, 278 (1995).
[23] D. A. DiCarlo, A. Sahni, and M. J. Blunt, Transp. Porous Media **39**, 347 (2000).
[24] K. K. Watson, Water Resour. Res. **2** (1966).
[25] T. Firincioglu, M. J. Blunt, and D. Zhou, Colloids Surf. A **155**, 259 (1999).
[26] A. Al Futaisi and T. W. Patzek, SPEJ **8**, 252 (2003).
[27] D. Zhou, M. J. Blunt, and F. M. Orr Jr., J. Colloid Interface Sci. **187**, 11 (1997).
[28] W. Rose, Transp. Porous Media **5**, 97 (1990).
[29] J. C. Bacri, M. Chaouche, and D. Salin, C. R. Acad. Sci. Paris **311**, 591 (1990).
[30] J.-L. Barrat and L. Bocquet, Phys. Rev. Lett. **82**, 4671 (1999)